Coupling of Edge-Element and Mode-Matching for Multistep Dielectric Discontinuity in Guiding Structures

Shanjia Xu and Xinquing Sheng

***Abstract*— A new approach is proposed for dielectric multistep discontinuity in guiding structures which combines edge-element analysis with the mode-matching method and multimode network theory. It is demonstrated that the approach has the generality of the edge-element analysis and the simplicity of the multimode network method, while retaining the high accuracy of the mode-matching method. The calculations for different multistep discontinuities verify the effectiveness and suitability of the approach for analysis of three-dimensional (3-D) lossy dielectric discontinuity problem.**

I. Introduction

The dielectric discontinuity problem is one of most basic practical problems in microwave engineering [1]–[4]. Of various discontinuity problems, multistep discontinuity has been recognized as a basic discontinuity problem in guiding structures. It is not only because most discontinuities in the planar circuit belong to this kind of problem, but also that many discontinuity problems can be approximated to this category with staircase approximation [5].

Many methods, such as the mode-matching method, the multimode network method, and the three-dimensional (3-D) finite element method have been developed to treat this kind of discontinuity problem [5]–[12]. It is well known that the mode-matching method is accurate, but it becomes very cumbersome for complicated discontinuity problems; it often suffers from the convergence problem due to truncated modal expansions [6]. To overcome this difficulty, an approach combining multimode network theory with the mode-matching method has been developed [7]–[9]. However, searching roots of the complex transcendental equation makes it inconvenient for solving lossy dielectric discontinuity problems. In recent years, the 3-D finite element method has been successfully used for solving discontinuity problems in guidance structures [10]–[13], but long computer time and large storage requirements limit its application.

A new approach is proposed in this paper for multistep dielectric discontinuity in guiding structures which combines edge-element analysis with the mode-matching method and multimode network theory. It is demonstrated that the approach has the generality of the edge-element analysis and the simplicity of the multimode network treatment while retaining the high accuracy of the mode-matching method. The calculations of the scattering characteristics for lossy dielectric block partially filled in the waveguide, and the semiconductor sample insert in the waveguide, verify the effectiveness and suitability of the approach.

II. Theoretical Analysis

As an example of multistep dielectric discontinuity without losing generality, Fig. 1 presents a structure of this kind of discontinuity with a complex dielectric constant of every segment. The solution procedure of the proposed approach could be divided into two steps: 1) analyze the eigenvalue problems of two waveguides at the two sides of each discontinuity in the transverse cross section with the edge element method; and 2) calculate the scattering characteristics of the whole discontinuity in the longitudinal direction with the mode-matching method combining with the multimode network theory.

Manuscript received June 11, 1995; revised October 18, 1996.

The authors are with the Department of Electronic Engineering and Information Science, University of Science and Technology of China, Hefei, 230027, China.

Publisher Item Identifier S 0018-9480(97)00837-5.

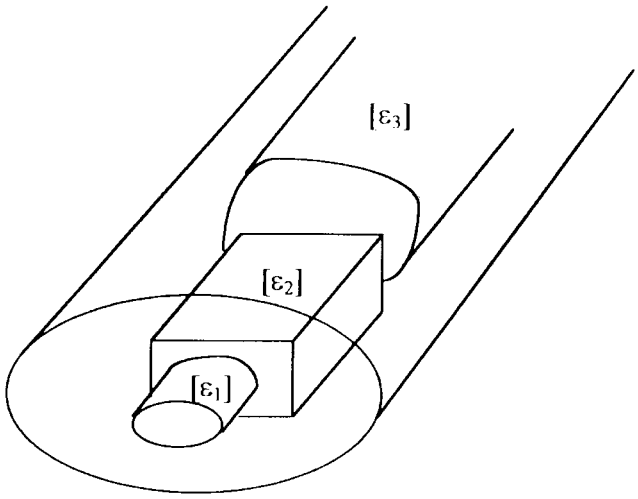

Fig. 1. Multistep discontinuity in guiding structure.

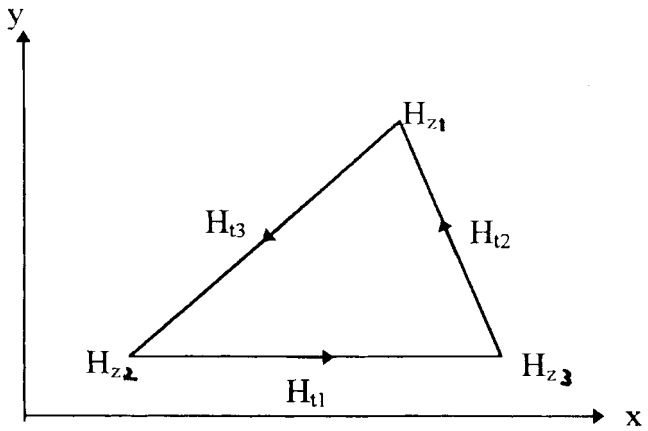

Fig. 2. Triangular edge element.

A. Analysis of Eigenvalue Problem with Edge-Element Method

It is well known that the eigenvalue problem of guided wave structures can be equivalent to the variational problem of the following functional:

$$F(\boldsymbol{H}) = \int\int_{\Omega} [(\nabla \times \boldsymbol{H})^* \cdot ([p]\nabla \times \boldsymbol{H}) - k_0^2[q]\boldsymbol{H}^* \cdot \boldsymbol{H}]\, dxdy \quad (1)$$

where k_0 is the vacuum wavenumber; $[p]$ and $[q]$ are described in detail in [14].

The full vector $\boldsymbol{H}$ is interpolated by the triangular edge element shown in Fig. 2 as

$$H_x^e = \{U\}^T\{H_t\}^e \quad (2)$$

$$H_y^e = \{V\}^T\{H_t\}^e \quad (3)$$

$$H_z^e = j\{N\}^T\{H_z\}^e \quad (4)$$

where T stands for transpose and e indicates the eth element, $\{H_t\}^e$ and $\{H_z\}^e$ are, respectively, composed of three side tangential

0018–9480/97$10.00 © 1997 IEEE

unknowns H_{t1}–H_{t3}, and three nodal axial unknowns H_{z1}–H_{z3}, and $\{U\}$, $\{V\}$, $\{N\}$ are the shape function vectors, which are defined all the same with those in [14].

Substituting (2)–(4) into (1), from variational principle, we obtain the following algebraic eigenvalue equations from which the propagation constant β can be directly obtained:

$$[A_{tt}]\{H_t\} = \beta^2[B_{tt}]\{H_t\} \tag{5}$$

where $[A_{tt}]$ and $[B_{tt}]$ are the same with those given in [14].

After obtaining the ith eigenvalue β_i and the corresponding transverse component $\{H_t\}_i$ from (5), the transverse magnetic eigenfunction of the ith mode can be expressed as

$$\boldsymbol{H}_{\mathbf{ti}} = A_i \sum_e [\{U\}^T \{H_t\}_i^e \mathbf{e_x} + \{V\}^T \{H_t\}_i^e \mathbf{e_y}]. \tag{6}$$

The longitudinal component $\{H_z\}_i$ of the ith eigenvector can be determined by

$$\{H_z\}_i = \beta [K_{zz}]^{-1}[K_{zt}]\{H_t\}_i. \tag{7}$$

Then, according to the Maxwell equations, the transverse electric component can be written as

$$\mathbf{E_t} = \frac{1}{j\omega\epsilon_0}\left[p_x\left(\frac{\partial H_z}{\partial y} - \frac{\partial H_y}{\partial z}\right)\mathbf{e_x} + p_y\left(\frac{\partial H_x}{\partial z} - \frac{\partial H_z}{\partial x}\right)\mathbf{e_y}\right] \tag{8}$$

namely:

$$\mathbf{E_t} = \frac{\omega\mu_0}{\beta}\frac{\beta}{jk_0^2}\left[p_x\left(\frac{\partial H_z}{\partial y} + j\beta H_y\right)\mathbf{e_x} + p_y\left(-j\beta H_x - \frac{\partial H_z}{\partial x}\right)\mathbf{e_y}\right] \tag{9}$$

and the transverse electric eigenfunction of the ith mode can be defined as

$$\mathbf{e_{ti}} = \frac{\beta_i}{jk_0^2}\left[p_x\left(\frac{\partial H_{zi}}{\partial y} + j\beta_i H_{yi}\right)\mathbf{e_x} + p_y\left(-j\beta_i H_{xi} - \frac{\partial H_{zi}}{\partial x}\right)\mathbf{e_y}\right]. \tag{10}$$

The above formulation can be discretized as

$$\mathbf{e_{ti}} = \frac{A_i\beta_i}{k_0^2}\sum_e [p_x(\{N_y\}^T\{H_z\}_i^e + \beta_i\{V\}^T\{H_t\}_i^e)\mathbf{e_x} - p_y(\{N_x\}^T\{H_z\}_i^e + \beta_i\{U\}^T\{H_t\}_i^e)\mathbf{e_y}]. \tag{11}$$

Here, $\{N_x\} = \frac{\partial}{\partial x}\{N\}$, $\{N_y\} = \frac{\partial}{\partial y}\{N\}$.

According to the above definition of the transverse electric eigenfunction, the characteristic impedance of the ith mode is determined by

$$Z_i = \frac{\omega\mu_0}{\beta_i}. \tag{12}$$

The amplitude A_i of the ith eigenfunction can be obtained from the following orthonormal relation:

$$\int_s \mathbf{e_{ti}} \times \mathbf{h_{tj}} \cdot d\mathbf{s} = \delta_{ij}. \tag{13}$$

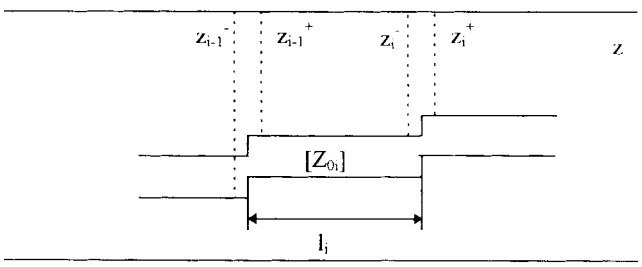

Fig. 3. The longitudinal section of a multistep discontinuity.

B. Impedance Transform Formulas

The transverse electric and magnetic fields in the waveguide on the left-hand side of the discontinuity can be expressed in terms of the superposition of the complete set of $\mathbf{e_{ti}}$, $\mathbf{h_{t_i}}$ as

$$\mathbf{E}_t = \sum_i \mathbf{e_{ti}} U_i \tag{14}$$

$$\boldsymbol{H}_{\mathbf{t}} = \sum_i \mathbf{h_{ti}} I_i. \tag{15}$$

Similarly, we have

$$\overline{\mathbf{E}}_{\mathbf{t}} = \sum_i \overline{\mathbf{e}}_{\mathbf{ti}} \overline{U}_i \tag{16}$$

$$\overline{\boldsymbol{H}}_{\mathbf{t}} = \sum_i \overline{\mathbf{h}}_{\mathbf{ti}} \overline{I}_i. \tag{17}$$

Here, the quantities with superbar indicate those on the right-hand side of the discontinuity. At the discontinuity plane, the tangential field components must be continuous. From (14) to (17), we obtain

$$\sum_i U_i \mathbf{e_{ti}} = \sum_i \overline{U}_i \overline{\mathbf{e}}_{\mathbf{ti}} \tag{18}$$

$$\sum_i I_i \mathbf{h_{ti}} = \sum_i \overline{I}_i \overline{\mathbf{h}}_{\mathbf{ti}}. \tag{19}$$

Cross multiplying (18) by $\mathbf{h_{ti}}$ from right and (19) by $\overline{\mathbf{e}}_{\mathbf{ti}}$ from left, then intergrating the resultant equations by invoking the orthonormal relation (13), we obtain

$$U_i = \sum_j Q_{ij}\overline{U}_j \tag{20}$$

$$\sum_j Q_{ji} I_j = \overline{I}_i \tag{21}$$

with

$$Q_{ij} = \int\int_s \overline{\mathbf{e}}_{\mathbf{ti}} \times \mathbf{h_{tj}} \cdot d\mathbf{s}. \tag{22}$$

Equations (20) and (21) may be written in matrix form as

$$\{U\} = [Q]\{\overline{U}\} \tag{23}$$

$$[Q]_t\{I\} = \{\overline{I}\}. \tag{24}$$

According to the definition of the impedance of the multimode network, we have

$$\{U\} = [Z]\{I\} \qquad \{\overline{U}\} = [\overline{Z}]\{\overline{I}\} \tag{25}$$

and the following impedance transform formula [5]:

$$[Z] = [Q][\overline{Z}][Q]_t. \tag{26}$$

C. Scattering Analysis of MultiStep Discontinuity

Fig. 3 shows the longitudinal section of a multistep discontinuity. It is known that the reflection coefficient matrix $[\Gamma(z_i^-)]$ at the $z = z_i^-$ plane looking to the right can easily be obtained as

$$[\Gamma(z_i^-)] = ([Z(z_i^-)] + [Z_{oi}])^{-1}([Z(z_i^-)] - [Z_{oi}]) \tag{27}$$

TABLE I
COMPARISONS OF THE TRANSMISSION CHARACTERISTICS FOR A SAMPLE WITH DIFFERENT GAPS BETWEEN DIFFERENT ANALYSIS METHODS

g mm	S_{21} multi-mode network method[11]		S_{21} present method	
	$\lvert s_{21}\rvert db$	ϕ_{21} degree	$\lvert s_{21}\rvert db$	ϕ_{21} degree
0.2	-2.68	-59.92	-2.78	-62.43
0.4	-2.45	-59.71	-2.48	-61.02
0.6	-2.29	-58.70	-2.28	-59.91
0.8	-2.15	-58.26	-2.16	-59.03
1.0	-2.03	-57.84	-2.05	-58.39
2.0	-1.60	-55.87	-1.58	-54.87
3.0	-1.27	-53.90	-1.23	-52.30
4.0	-1.01	-51.71	-0.92	-49.43
5.0	-0.78	-49.10	-0.74	-47.35

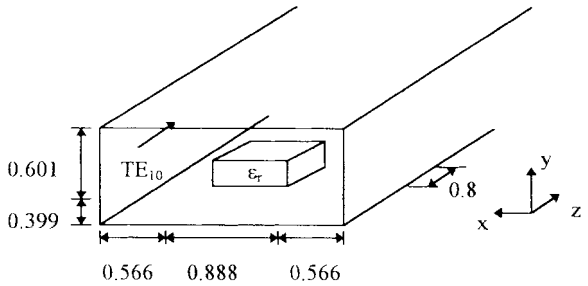

Fig. 4. Rectangular dielectric scattering obstacle in a waveguide.

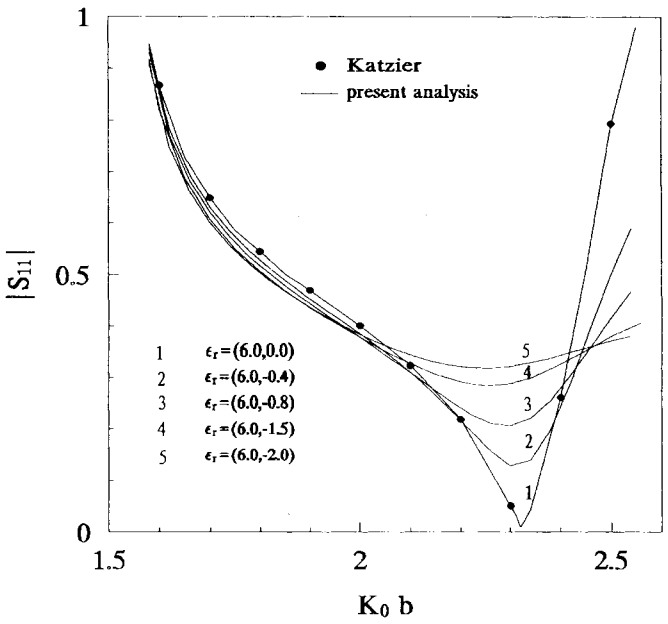

Fig. 5. Reflection characteristics of a dielectric-loaded waveguide.

where $[Z(z_i^-)]$ is the input impedance matrix at the $z = z_i^-$ plane, determined by (26), and $[Z_{oi}]$ is the characteristic impedance matrix of the ith step discontinuity. Then, the input impedance matrix at the $z = z_{i-1}^-$ plane looking to the right is determined by the impedance transform technique as [5]

$$[Z(z_{i-1}^+)] = [Z_{oi}]([I] + [H_i][\Gamma(z_i^-)][H_i]) \cdot ([I] - [H_i][\Gamma(z_i^-)][H_i])^{-1} \quad (28)$$

where $[H_i]$ is the phase matrix of the ith step discontinuity. $[Z_{oi}]$ and $[H_i]$ are all diagonal matrices, and their elements are, respectively, given as

$$[Z_{oi}]_{mn} = \delta_{mn}\omega\mu/\beta_{in} \quad (29)$$

$$[H_i]_{mn} = \delta_{mn}\exp(-j\beta_{in}l_i). \quad (30)$$

Here, β_{in} is the propagation constant of the nth mode in the dielectric waveguide of the ith section. Thus, the total reflection coefficient matrix of the multistep discontinuity can be determined by using (26)–(30) several times.

D. Symmetrical Consideration of the Structure

For a symmetrical discontinuity structure in the longitudinal direction, the scattering of a guided mode may be analyzed in terms of the symmetrical and antisymmetrical excitations for which we have the open-circuit (OC) and short-circuit (SC) bisection, respectively, as previously had [7]. The reflection coefficient for each guided mode at the symmetrical plane is 1.0 for the OC bisection or -1.0 for the SC bisection. Let $[R_o]$ and $[R_s]$ be the reflection coefficient matrices at the incident plane for the OC and the SC bisection, respectively; the guided mode reflection coefficient matrix $[R]$ and the transmission matrix $[T]$ of the entire symmetrical structure are then given by

$$[R] = ([R_0] + [R_s])/2 \quad (31)$$

$$[T] = ([R_0] - [R_s])/2. \quad (32)$$

For the dominant mode, the scattering parameters $S_{21} = S_{12}$ and $S_{11} = S_{22}$ are determined from the first row and first column of the

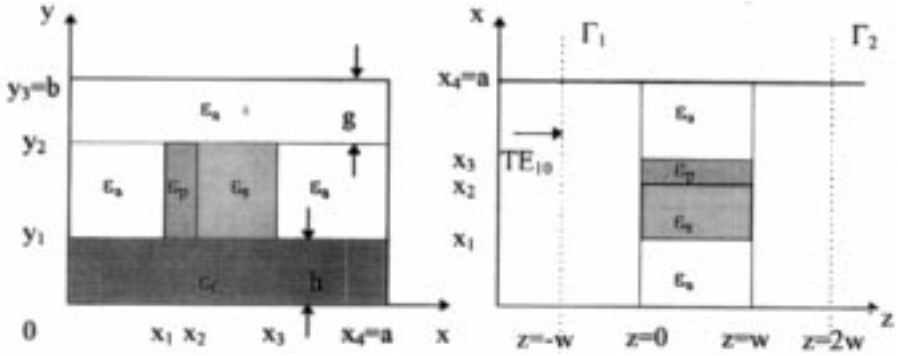

Fig. 6. Cross section of the stratified lossy dielectric block in the rectangular waveguide.

$[R]$ and $[T]$ matrices, respectively, as

$$S_{11} = R(1, 1) = \frac{1}{2}[R_0(1, 1) + R_s(1, 1)] \tag{33}$$

$$S_{21} = T(1, 1) = \frac{1}{2}[R_0(1, 1) - R_s(1, 1)]. \tag{34}$$

III. Numerical Examples

In order to verify the effectiveness and the accuracy of the present approach, we have analyzed two 3-D dielectric discontinuity problems. The first problem calculated is a rectangular dielectric scattering obstacle placed in a waveguide as shown in Fig. 4. Fig. 5 shows the magnitude of reflection coefficient $|s_{11}|$ versus the normalized frequency $k_0 b$ with the complex relative permittivity as parameters. It can be seen from Fig. 5 that the reflection coefficients for lossless case obtained by our approach, shown by the solid line, agree very well with the results of [15], shown by dots. Also, Fig. 5 shows that the larger the loss of the dielectric material, namely, the larger the imaginary part of the dielectric constant, the weaker the resonant phenomenon in the passband, as expected. Thus, the effectiveness and the accuracy of the present approach are justified. In our calculation, a total of 153 nodes are used in the analysis of eigenvalue problem with the edge-element method, 40 eigenmodes in the empty waveguide, and 5 eigennodes in the dielectric-loaded waveguide are included in the mode-matching procedure. The whole computing time for this structure requires only 3 min for every frequency with a 486 personal computer.

The second problem analyzed is a semiconductor sample inserted in the rectangular waveguide as shown in Fig. 6, which was used to determine the conductivity of the semiconductor by means of contactless microwave technology [7], [8]. The sample, together with its mounting structure, is actually a stratified lossy dielectric block. Table I shows the comparisons of the transmission characteristics of a semiconductor sample with different gaps g between the results obtained with the multimode network method [7] and with the present approach. The physical parameters of the sample are, respectively, $\epsilon_p = (-41, -1816)$ (dielectric constant of semiconductor epitaxial layer), $\epsilon_s = (11, -0.8)$ (dielectric constant of subtract), $Y_2 - Y_1 = 0.002$ mm (thickness of the epitaxial layer), $Y_3 - Y_2 = 1$ mm (thickness of the substrate), and $w = 5$ mm (length of the sample), while the data of the mounting structure are $h = 0$, $\epsilon_a = \epsilon_b = \epsilon_w = 1.0$, $Y_1 = 11.53$, $a = 22.86$ mm, and $b = 10.16$ mm. The good agreement between the different methods can be found in Table I. Again, the effectiveness of the approach is verified.

IV. Conclusion

The multistep dielectric discontinuity problem has been analyzed by a new approach which combines edge-element analysis with mode-matching method and multimode network theory. Our practice reveals that the approach has the generality of the edge-element analysis and the simplicity of the multimode network technique, while retaining the high accuracy of the mode-matching method. The calculations of the scattering properties for lossy dielectric block partially filled in the waveguide, and the semiconductor segment with mounting structure places in the waveguide, verify the effectiveness and the accuracy of the present approach.

References

[1] N. Marcuvitz, *Waveguide Handbook.* London, U.K.: Peregrinus, 1986.
[2] K. Chang and P. J. Khan, "Analysis of a narrow capacitive strip in waveguide," *IEEE Trans Microwave Theory Tech.*, vol. MTT-22, pp. 536–541, May 1974.
[3] H. B. Chu and K. Chang, "Analysis of a wide resonant strip in waveguide," *IEEE Trans. Microwave Theory Tech.*, vol. 40, pp. 495–498, Mar. 1992.
[4] A. Rong, "Discontinuities of E-plane strip with partial height and their application to millimeter wave filters," *J. Appl. Sciences*, vol. 8, pp. 10–18, Jan. 1990.
[5] S. Xu, S. T. Peng, and F. K. Schwering, "Effect of transition waveguides on dielectric waveguide directional couplers," *IEEE Trans. Microwave Theory Tech.*, vol. 37, pp. 686–690, Apr. 1989.
[6] R. Mitra and S. W. Lee, *Analytical Techniques in the Theory of Guided Waves.* New York: Macmillan, 1971.
[7] S. Xu, X. Wu, P. Greiner, C. R. Becker, and R. Geick, "Microwave transmission and reflection of stratified lossy dielectric segment partial filled waveguide," *Int. J. Inf. Millim. Waves*, vol. 13, no. 4, pp. 569–587, 1992.
[8] S. Xu, X. Wu, P. Boege, H. Schafer, C. R. Becker, and R. Geick, "Scattering characteristics of 3-D discontinuity consisting of semiconductor sample filled in waveguide with gaps," *Int. J. Infrared Millim. Waves*, vol. 14, no. 10, pp. 2155–2190, 1993.
[9] S. Xu, X. Sheng, P. Greiner, C. R. Becker, and R. Geick, "High-order finite-element analysis for scattering characteristics of II-VI semiconductor materials," *Chin. J. Infrared Millim. Waves*, vol. 12, no. 3, pp. 177–184, 1992.
[10] J. P. Webb, G. L. Maile, and R. L. Ferrari, "Finite-element solution of three-dimensional electromagnetic problems," *Proc. Inst. Elect. Eng.*, vol. 130, pt. H, pp. 153–159, Mar. 1983.
[11] K. Ise, K. Inoue, and M. Koshiba, "Three-dimensional finite-element solution of dielectric scattering obstacles in a rectangular waveguide," *IEEE Trans. Microwave Theory Tech.*, vol. 38, pp. 1352–1359, Sept. 1990.
[12] ——, "Three-dimensional finite-element method with edge-elements for electromagnetic waveguide discontinuities," *IEEE Trans. Microwave Theory Tech.*, vol. 39, pp. 1289–1294, Aug. 1991.
[13] S. Xu and X. Sheng, "Automatic division technique for 3-D finite element," *Acta Electron. Sin.*, vol. 22, pp. 79–82, June 1994.
[14] M. Koshiba and K. Inoue, "Simple and efficient finite-element analysis of microwave and optical waveguides," *IEEE Trans. Microwave Theory Tech.*, vol. 40, pp. 371–377, Feb. 1992.
[15] H. Katzier, "Strenvrhalten elektromagnetischer wellen bei sprunghaften ubergangen geschirmter dielektrischer leitungen," *Arch. Elektron. Ubertrag. Tech.*, vol. 38, pp. 290–296, 1984.